Published in final edited form as:
Water Res. 2020 February 01; 169: 115240. doi:10.1016/j.watres.2019.115240.

Hydroxyl radical scavenging by solid mineral surfaces in oxidative treatment systems: Rate constants and implications

Klara Rusevova Crincoli[a], **Scott G. Huling**[b,*]

[a]National Research Council, R.S. Kerr Environmental Research Center, 919 Kerr Lab Dr., Ada, OK, 74820, USA

[b]U.S. Environmental Protection Agency, Office of Research and Development, National Risk Management Research Laboratory, Robert S. Kerr Environmental Research Center, 919 Kerr Lab Dr., Ada, OK, 74820, USA

Abstract

Advanced oxidation treatment processes used in various applications to treat contaminated soil, water, and groundwater involve powerful radical intermediates, including hydroxyl radicals (•OH). Inefficiency in •OH-driven treatment systems involves scavenging reactions where •OH react with non-target species in the aqueous and solid phases. Here, •OH were generated in iron (Fe)- and UV-activated hydrogen peroxide (Fe-AHP, UV-AHP) systems where the loss of rhodamine B served as a quantitative metric for •OH activity. Kinetic analysis methods were developed to estimate the specific •OH surface scavenging rate constant ($k_{\equiv S}$). In the Fe-AHP system, $k_{\equiv S}$ for silica (2.85×10^6 $1/m^2 \times s$) and alumina (3.92×10^6 $1/m^2 \times s$) were similar. In the UV-AHP system, estimates of $k_{\equiv S}$ for silica (4.50×10^6 $1/m^2 \times s$) and alumina (7.45×10^6 $1/m^2 \times s$) were higher. $k_{\equiv S}$ for montmorillonite (MMT) in the UV-AHP systemwas $\leq 4.22 \times 10^5$ $1/m^2 \times s$. Overall, $k_{\equiv S,silica} \sim k_{\equiv S,\ alumina} > k_{\equiv S,MMT}$ indicating $k_{\equiv S}$ is mineral specific. Radical scavenging was dominated by surface scavenging at 10–50 g/L silica, alumina, or MMT, in both Fe-AHP and UV-AHP systems. The experimentally-derived surface •OH scavenging rate constants were extended to in-situ chemical oxidation (ISCO) treatment conditions to contrast •OH reaction rates with contaminant and aqueous phase reactants found in aquifer systems. •OH reaction was dominated by solid surfaces comprised of silica, alumina, and montmorillonite minerals relative to •OH reaction with trichloroethylene, the target compound, and H_2O_2, a well-documented radical scavenger. These results indicate that solid mineral surfaces play a key role in limiting the degradation rate of contaminants found in soil and groundwater, and the overall treatment efficiency in ISCO systems. The aggressive •OH scavenging measured was partially attributed to the relative abundance of scavenging sites on mineral surfaces.

*Corresponding author. huling.scott@epa.gov (S.G. Huling).

Declaration of competing interest

The authors declare that they have no known competing financial interests or personal relationships that could have appeared to influence the work reported in this paper.

Appendix A. Supplementary data

Supplementary data to this article can be found online at https://doi.org/10.1016/j.watres.2019.115240.

Keywords

Hydroxyl radicals; Surface scavenging; Mineral surfaces

1. Introduction

Advanced oxidation treatment processes, used in various applications to treat contaminated soil, water, and groundwater involve powerful radical intermediates, including hydroxyl radicals (•OH). Inefficiency in oxidative treatment processes involving radical intermediates is attributed to two main mechanisms, radical scavenging and nonproductive reactions (NPR). Radical scavenging involves the reaction of free radicals with non-target chemical species; and NPR involve reactions that deplete the source of oxidant which in turn diminishes radical production. Radical scavengers may either be soluble and react with radicals in the aqueous phase or may be present as solids and react on the surfaces of solid phase media. Kinetic studies of •OH scavenging in oxidative treatment processes have predominantly been focused on soluble constituents in the aqueous phase and have not addressed radical scavenging by solid phase media also found in oxidative treatment systems. The focus of this study was to quantify radical scavenging by solid surfaces.

Hydrogen peroxide (H_2O_2)-driven processes serve as the basis for different oxidative treatment applications including in situ chemical oxidation (ISCO) of contaminated aquifers (Huling and Pivetz, 2006; Siegrist et al., 2011), and advanced oxidation processes for water and wastewater treatment (Bautista et al., 2008; Babuponnusami and Muthukumar, 2014). Oxidative systems based on iron (Fe)-activated hydrogen peroxide (R1-R3, R9; Table 1) generate •OH, which are powerful and indiscriminate free radicals that react with a wide array of environmentally relevant contaminants (Buxton et al., 1988; Haag and Yao, 1992). At pH ≥4, the efficiency of •OH-driven contaminant transformations in heterogeneous systems can be significantly limited due to the reduction of H_2O_2 to O_2 via a two e^- transfer, non-radical pathway on the iron surface (Remucal and Sedlak, 2011), and/or from catalyst precipitation (Pignatello et al., 2006).

The rates of •OH reaction with non-target chemical species (S_i) in the aqueous phase have been determined in well-characterized, homogeneous, aqueous systems (Kwan and Volker, 2003; Grebel et al., 2010). Such calculations utilize published second-order rate constants (Buxton et al., 1988; Haag and Yao, 1992) and scavenger concentrations ($[S_i]$). Here, rhodamine B dye (RhB) was the target compound (R4, Table 1); and S_i are either from anthropogenic sources (e.g. H_2O_2) or are naturally occurring (e.g. HCO_3^-, CO_3^{2-}) (R5-R6, Table 1). In complex heterogeneous systems involving both aqueous and solid phases, calculation of •OH scavenging rates must also include reaction rates between •OH and the solid phase materials (R7, Table 1). Radical scavenging by solid phase surfaces has been acknowledged (Huling et al., 1998; Miller and Valentine, 1999; Kwan and Volker, 2003; Rusevova et al., 2012) but still has not been quantified. Consequently, several fundamental issues have not been addressed, including the extent to which solid surfaces scavenge radicals, whether the rate of radical scavenging by solid surfaces is significant relative to

aqueous phase scavenging, and whether radical scavenging by solid surfaces is mineral-dependent.

Studies investigating H_2O_2 activation and contaminant transformation efficiency in heterogeneous systems have examined a broad array of minerals, soils, and aquifer materials (Miller and Valentine, 1999; Petigara et al., 2002; Xu and Thomson, 2010); iron oxides including goethite, ferrihydrite, pyrite or magnetite (Huang et al., 2001; Kwan and Volker, 2002; Baldrian et al., 2006; Matta et al., 2007, Rusevova et al., 2012); and various Fe-containing aluminosilicates (Luo et al., 2009; Garrido-Ramirez et al., 2010). Factors influencing H_2O_2 activation, NPR, and/or •OH scavenging include the Fe and Mn content of the aquifer materials, organic matter and microbial enzymes (Petigara et al., 2002; Xu and Thomson, 2010), mineral surface area, particle size, coordination chemistry, and crystallinity (Huang et al., 2001; Hermanek et al., 2007). Reactants responsible for NPR include manganese oxides and some mineral forms of iron (R8, Table 1) (Remucal and Sedlak, 2011), which are commonly found in environmental systems. Quantifying radical scavenging by solid surfaces in heterogeneous systems and recognizing NPR are key requirements in a complete understanding of contaminant transformation efficiency.

The objectives of this study were to develop kinetic analysis and laboratory methods to estimate surface radical scavenging rate constants that can be used to differentiate between radical scavenging in the aqueous and solid phases; quantify radical scavenging by mineral-specific solid phase media; and to assess the relative rates of radical scavenging by dissolved and solid phase scavenging species.

2. Model development and experimental

In the development of the kinetic analysis model, three reaction conditions are considered where; (1) the solid phase media does not react with H_2O_2, (2) the solid phase media reacts with H_2O_2 but does not produce •OH (i.e., nonproductive reactions), and (3) the solid phase media reacts with H_2O_2, forms •OH, and may also involve nonproductive reactions. Here, methods of kinetic analysis were developed to estimate •OH scavenging rate constants for solid surfaces in oxidative treatment systems for conditions 1 and 2.

Alumina (Al_2O_3), silica (SiO_2), and montmorillonite (MMT) ($Al_2H_2O_{12}Si_4$) are solid phase minerals commonly found in soil and aquifer systems (Schwarzenbach et al., 2003). Alumina and silica are used as catalyst support media in oxidative treatment systems (Pham et al., 2009; Navalon et al., 2010; Sheng et al., 2017) representing potential radical scavenging media. Preliminary studies indicated silica and alumina were unreactive with H_2O_2, and montmorillonite (MMT) reacted with H_2O_2, but did not form •OH. These minerals were selected as potential solid phase radical scavengers.

The basis of the kinetic analysis was to contrast treatment results between simple, solids-free homogeneous oxidation systems and more complex, heterogeneous systems containing mineral species (R8-R9, Table 1). The homogeneous system was based on iron (Fe)-activated H_2O_2 reactions (Fe-AHP) (R1-R6, Table 1) and ultraviolet light (UV)-activated H_2O_2 (UV-AHP) reactions (R4-R6, R10, Table 1). The heterogeneous systems involved

identical treatment conditions as the homogeneous system but were amended with solid phase media. Consequently, differences in the loss of the probe were attributed to •OH scavenging by suspended solids in the Fe-AHP and UV-AHP treatment systems.

2.1. Probe selection

A non-volatile, hydrophilic probe that adsorbs poorly to solid phase media was required to minimize non-oxidative losses and to simplify the kinetic analysis. Several probes were tested and rhodamine B dye (RhB) was found to meet the criteria. RhB occurs in cationic and zwitterionic forms (Supporting Information (S) S.1; Figure S1) and was analyzed spectrophotometrically allowing rapid processing of samples which eliminated a quenching step of the H_2O_2.

2.2. Development of kinetic analysis methods

The rate of •OH accumulation is calculated as the difference between the rates of •OH production (P_{OH}) and •OH consumption (C_{OH}) (Eq. (1)) (Huling et al., 2001). •OH are highly reactive and a quasi-steady state approximation for •OH is assumed where d [OH]/dt ~ 0, and $C_{OH} \sim P_{OH}$ (Eq. (2)). Rhodamine B (RhB) was used as a probe and as a quantitative metric for •OH activity. The least-square regression of semi-logarithmic plots of RhB concentration versus time were linear indicating that •OH concentrations were at steady-state ($[OH]_{SS}$) and were used to determine the pseudo-first order degradation rate constants for RhB (k_{RhB}). The overall rate of •OH consumption (Eq. (3)) is the sum of rates of •OH reaction with the probe (R_P) (Eqs. (4) and (5)), scavengers in the aqueous phase, R_S (Eqs. (6) and (7)), and scavengers in the solid phase, $R_{\equiv S}$ (Eqs. (8) and (9)). The individual aqueous and solid phase scavengers are grouped into terms k_S and $k_{\equiv S}$, respectively. Equations (4) and (5) were combined and used to estimate $[\bullet OH]_{SS}$ (Eq. (10)), where k_4 was obtained from the literature (Table 1), and k_{RhB} was derived from laboratory data.

$$d[\bullet OH]/dt = P_{OH} - C_{OH} \quad \text{Eq. 1}$$

$$C_{OH} \sim P_{OH} \quad \text{Eq. 2}$$

$$C_{OH} = Rp + Rs + R_{\equiv S} \quad \text{Eq. 3}$$

$$Rp = k_4[RhB]\ [\bullet OH]_{SS} \quad \text{Eq. 4}$$

$$Rp = k_{RhB}\ [RhB] \quad \text{Eq. 5}$$

$$R_s = \Sigma_{i=1}^{n}\ k_i[S_i]\ [\bullet OH]_{SS} \quad \text{Eq. 6}$$

$$Rs = k_S\ [\bullet OH]_{SS} \quad \text{Eq. 7}$$

$$R_{\equiv S} = \Sigma_{i=1}^{n} k_{\equiv,i} [S_{\equiv,i}] S_A m_S [\bullet OH]_{SS} \quad \text{Eq. 8}$$

$$R_{\equiv S} = k_{\equiv S} S_A m_S [\bullet OH]_{SS} \quad \text{Eq. 9}$$

$$[\bullet OH]_{SS} = k_{RhB}/k_4 \quad \text{Eq. 10}$$

where,

P_{OH}, C_{OH} rates of •OH production and reaction, respectively (mol/L × s);

Rp, Rs, $R_{\equiv S}$ •OH reaction rates with the probe (RhB), scavengers in the aqueous phase (S_i), and surface scavengers ($S_{\equiv,i}$), respectively (mol/L × s);

$[\bullet OH]_{SS}$ pseudo-steady state hydroxyl radical concentration (mol/L);

[RhB] rhodamine B concentration (mol/L);

k_4 second order degradation rate constant of the RhB probe (L/mol × s);

k_{RhB} pseudo-first order degradation rate constant for RhB probe (1/s);

k_S sum of products of individual aqueous phase scavengers (S_i) and respective •OH reaction rate constants (k_i) (L/mol × s);

k_i second order rate constant of individual aqueous phase scavenger (L/mol × s);

$[S_i]$ individual aqueous phase scavenger concentration (mol/L);

$k_{\equiv S}$ surface scavenging rate constant, sum of products of individual solid phase scavengers ($S_{\equiv,i}$) and respective •OH reaction rate constants ($k_{\equiv,i}$) ($1/m^2 \times s$);

$k_{\equiv,i}$ specific second order rate constant of individual solid phase scavenger (L/mol × s);

$[S_{\equiv,i}]$ individual specific solid phase scavenger concentration (mol/L × m^2);

S_A surface area of the solid phase media (i.e., mineral) (m^2/g); and m_S mass of solid phase mineral (g).

2.2.1. Minerals unreactive with H_2O_2—The kinetic analysis method used to estimate $k_{\equiv S}$ involved contrasting results between a solids-free, homogeneous system and a solids-amended, heterogeneous system. Alumina and silica were found to be unreactive with H_2O_2 and were incrementally amended to the test reactors to determine if they played a role in surface scavenging of •OH. Eqs. (1)–(10) formed the basis to solve for P_{OH} (Eq. (11)). In an oxidative system without surface scavenging (i.e., mineral-free), the surface scavenging term in Eq. (11) is eliminated (Eq. (12)). In this case, the subscripts in Eqs. (11) and (12) represent 0 and 10 g/L, respectively, for either alumina or silica.

$$P_{OH,10} = k_4[RhB][\bullet OH]_{SS,10} + k_s[\bullet OH]_{SS,10} + k_{\equiv s} S_A m_{s,10}[\bullet OH]_{SS,10} \quad \text{Eq. 11}$$

$$P_{OH,0} = k_4[RhB]\,[\bullet OH]_{SS,0} + k_S[\bullet OH]_{SS,0} \quad \text{Eq. 12}$$

The experimental method used to differentiate between •OH scavenging in the solid phase and aqueous phase required two identical test conditions where one reactor was mineral-free and the other was amended with the alumina or silica minerals. The mineral-free, base case system contained Fe^{3+} ($[Fe^{3+}]_0$ = 0.18 mM), H_2O_2 ($[H_2O_2]_0$ = 29.4 mM), and RhB ($[RhB]_0$ = 1.04×10^{-2} mM), and the mineral-amended system contained the same concentrations of these reaction species, and alumina (1–50 g/L) or silica (1–g/L). The $[Fe^{3+}]_0$, $[H_2O_2]_0$, and $[RhB]_0$ were identical in both systems indicating that P_{OH} and k_S were also similar. The pseudo-first order degradation rate constant for H_2O_2 (k_{H2O2}), and the H_2O_2 loss over the duration of the experiments were determined and found to be similar between the mineral-free and mineral-amended treatment systems. Therefore, time-dependent differences in [RhB] were attributed to surface scavenging effects in the mineral-amended system. The steady state •OH concentrations for both systems, $[OH]_{SS,0}$, $[OH]_{SS,10}$ were determined experimentally (Eq. (10)); and the pseudo-first order reaction rate constants for RhB in mineral-free ($k_{RhB,0}$ (1/s)) and 1–50 g/L mineral-amended (e.g., $k_{RhB,10}$ (1/s); 10 g/L) systems were determined via semi-log plots of [RhB] versus time. On this basis, the rate of •OH production is similar between systems, allowing equations (11) and (12) to be set equal and permitting the surface scavenging rate constant, $k_{\equiv S}$, to be determined (Eq. (13)).

$$k_{\equiv s} = \frac{(([\bullet OH]_{SS,0})(k_4[RhB]) + k_s) - ([\bullet OH]_{SS,10}(k_4[RhB]) + k_S)}{S_A m_{S,10}[\bullet OH]_{SS,10}} \quad \text{Eq. 13}$$

A minor modification of this method was developed to estimate $k_{\equiv S}$ from the results of two mineral-amended oxidative systems containing different quantities of solid phase media. Eq. (11) was written for P_{OH} in reactors containing different quantities of alumina or silica minerals where subscripts 1 and 10, for example, represent 1 g/L and 10 g/L, respectively, for the solid phase media (Eqs. (14) and (15)). As before, time-dependent differences in [RhB] are attributed to surface scavenging with respect to differing quantities of solid phase media in the system.

$$P_{OH,1} = k_4[RhB][\bullet OH]_{SS,1} + k_S[\bullet OH]_{SS,1} + k_{\equiv S} S_A m_{S,1}[\bullet OH]_{SS,1} \quad \text{Eq. 14}$$

$$P_{OH,10} = k_4[RhB]\,[\bullet OH]_{SS,10} + k_S[\bullet OH]_{SS,10} + k_{\equiv S}\ S_A\ m_{S,10}\ [\bullet OH]_{SS,10} \quad \text{Eq. 15}$$

The rate constants for RhB in the 1 and 10 g/L mineral-amended systems ($k_{RhB,1}$ (1/s) and $k_{RhB,10}$ (1/s)), and the steady state •OH concentrations for both systems (i.e., $[OH]_{SS,1}$, $[OH]_{SS,10}$) (Eq. (10)), were determined. k_4, k_S, $[Fe^{3+}]_0$, $[H_2O_2]_0$, and $[RhB]_0$ were identical between the two systems indicating that P_{OH} and k_S were also similar. On this basis, the rate

of •OH production was similar between systems, allowing equations (14) and (15) to be set equal to solve for the surface scavenging rate constant, $k_{\equiv S}$ (Eq. (16)).

$$k_{\equiv S} = \frac{([\bullet OH]_{SS,10}(k_4[RhB] + k_S)) - ([\bullet OH]_{SS,1}(k_4[RhB] + k_S))}{(S_A m_{S,1}[\bullet OH]_{SS,1}) - S_A m_{S,10}[\bullet OH]_{SS,10}} \quad \text{Eq. 16}$$

2.2.2. Mineral reactive with H_2O_2—Preliminary testing using control reactors comprised of H_2O_2, RhB, and montmorillonite (MMT) showed that MMT was reactive with H_2O_2, but no loss in RhB was measured indicating that •OH were not formed (i.e., NPR). MMT was incrementally amended to test reactors in the UV-AHP oxidative treatment system to determine if MMT scavenged •OH. NPR were problematic in the determination of $k_{\equiv S}$ because the H_2O_2 loss from NPR represented a potential loss in H_2O_2 for productive reactions, relative to the MMT-free, baseline system (i.e., UV/H_2O_2, RhB). Consequently, differences in P_{OH} between the MMT-amended and the MMT-free systems could invalidate the assumption used in the development of Eq. (13) (i.e., $P_{OH,MMT\text{-}free} = P_{OH,MMT\text{-}amended}$). In the MMT-amended system where NPR played a role, the estimated value of $[\bullet OH]_{SS,10}$ was projected to be at a minimum due to the loss of H_2O_2. Under this condition, the corresponding estimate of $k_{\equiv S}$ represents the maximum estimated value (i.e., Eq. (13)). In an ideal system where NPR and H_2O_2 loss did not play a role, higher estimates of $[OH]_{SS,10}$ would result, and estimated values for $k_{\equiv S}$ (Eq. (13)) would decrease relative to the actual MMT-amended system. Therefore, in the MMT-amended systems evaluated in this study, estimates of $k_{\equiv S}$ represent a maximum value and are therefore reported as less than or equal to (≤). Overall, bracketing the maximum value of $k_{\equiv S}$ in MMT-amended systems in this manner allows the comparison of $k_{\equiv S}$ results between MMT, silica, and alumina.

2.3. Materials

The chemicals used in this study were reagent grade and used as received. Rhodamine B (RhB) (21.33% w/w) was purchased from Turner Designs, $Fe(NO_3)_3 \cdot 9H_2O$ and H_2O_2 (30% w/w) were from Aldrich, and titanium sulfate ($TiSO_4$) was from Pfaltz and Bauer Inc. Sources of alumina (α phase) and silica were obtained from Aldrich and the US Department of Commerce, National Institute of Standards and Technology, respectively. The calcium-based montmorillonite (MMT) (Apache County, AZ) was from the Clay Minerals Society. The minerals were not subjected to physical or chemical pre-treatment and were used as received. All glassware and containers were acid-washed and rinsed with deionized (DI) water before use.

2.4. Batch experiments

Test reactors were carried out at room temperature (21 °C) in borosilicate glass vessels (40 mL) with Teflon-coated screw caps. In the base-case homogeneous Fe-AHP oxidation test system (25 mL total volume), chemical addition and initial concentrations were RhB (5 mg/L; 1.04×10^{-2} mM), Fe^{3+} (10 mg/L; 0.18 mM), and H_2O_2 (1000 mg/L; 29.4 mM). In the heterogeneous Fe-AHP systems, the same procedures were used except silica (1–30 g/L) or alumina (1–50 g/L) solid phase media were amended. Solutions of Fe^{3+} were prepared daily and over the short reaction period (1 h), neither time nor conditions permitted

geomorphologic changes that would account for changes in the H_2O_2 reaction mechanism, as observed by others (Kwan and Volker, 2002). These conditions were designed and used specifically to assure that the H_2O_2 reaction and •OH formation was similar between solids-free and solids-amended systems. A UV-AHP reaction system was developed as a second method and used to estimate $k_{\equiv S}$ of the silica, alumina, and MMT minerals. In this Fe-free method, H_2O_2 activation and •OH formation occurred in the aqueous phase using a UV Lamp (High-Performance UVP Transilluminator, Model TFM-20) containing 4 UV-A tube bulbs (25 W bulbs, 115 V, 60 Hz, 2.0 amps, 365 nm wavelength). The UV-activated H_2O_2 test conditions were similar as the Fe-AHP test conditions described above, but without the addition of Fe^{3+}. In the heterogeneous system, silica (1–10 g/L), alumina (1–50 g/L), or MMT (1–50 g/L) solid phase media were amended. Uncovered test reactors were placed under the UV light lamp. The initial concentration of RhB and H_2O_2 were established such that there was approximately equal reaction with •OH (i.e., $k_6 \times [H_2O_2] = k_4 \times [RhB]$, where k_6 and k_4 are 2.7×10^7 1/M × s and 2.5×10^{10} 1/M × s, respectively (Buxton et al., 1988)). Reaction pH was monitored but not adjusted to eliminate the potential addition of scavengers into the reaction system. Complete-mix batch reactors were continuously stirred (500 rpm) on a magnetic stirrer (10-spot magnetic stirrer; SCILOGEX MS-H-S10) over the course of the experiment; and the reaction pH, [RhB], and $[H_2O_2]$ were monitored over the course of the reaction period. Prior to analysis, aqueous samples were separated from suspended solid phase media by centrifugation (Eppendorf Minispin; 3000 rpm; 2 min).

2.5. Solids characterization and analytic methods

Specific surface area (SSA) of the minerals was determined by the BET method using N_2 adsorption-desorption isotherms measured on Quantachrome NOVA 4200e (Boynton Beach, FL). Metals concentrations in Al_2O_3, SiO_2, and MMT were determined by inductively coupled plasma, optical emission spectroscopy (ICP-OES) using PerkinElmer Optima 8300DV ICP-OES, based on EPA Method 200.7. The mineral samples (n = 3) were extracted by microwave digestion in a 10% HNO_3 solution. The suspension was sealed in a pressurized liner and microwaved (175 °C). After digestion, the solids settled overnight prior to analysis, or were filtered (0.45 μm membrane filter) if solids remained in suspension. The ICP-OES detection limit and quantitation limit for Fe and Mn were 4.0 and 8.1 mg/kg, respectively. Quality control results for the calibration checks, method blanks, digestion blanks, interference checks, digestion duplicates, and serial dilutions met criteria established in EPA Method 200.7 (US EPA, 1994). Filtered solutions of alumina, silica, and MMT suspensions (50 g/L) were analyzed for Cl^- and Br^- using Lachat flow injection analyzers (FIA) where the MDL was 0.048 mg/L for Br^-, and 0.574 mg/L for Cl^-. Suspensions (10 g/L) of alumina and silica were prepared and acidified, as done in the batch experiments above, and analyzed for dissolved species including silica (as $[Si]_{AQUEOUS}$) using ICP OES. The solution was decanted, the solids were re-suspended, acidified, and re-analyzed for $[Si]_{AQUEOUS}$ to assess whether continuous leaching from the solid phase media into the aqueous phase occurs. Mineral composition analysis was determined using the Rigaku MiniFlex X-ray diffractometer which provides a qualitative identification of minerals present in solid matrices and is based on a comparison to reference diffraction data for known compounds (S.2).

H_2O_2 was measured using a modified peroxytitanic acid colorimetric procedure. Dilutions of the aqueous samples were amended with $TiSO_4$ (100 μL) and absorbance of the H_2O_2-$TiSO_4$ complex (λ_{max} = 407 nm) was measured (n = 2) on the Jenway 6505 UV/Visible spectrophotometer. Similarly, the absorbance of ferrous (Fe^{2+}) and total iron (Fe^{2+}, Fe^{3+}) (λ_{max} = 510 nm) (n = 2), using the Phenanthroline Method (APHAAWWA et al., 1989) and RhB (λ_{max} = 556 nm) were determined (n = 3) spectrophotometrically on the Jenway 6505. Regression analysis of the spectrophotometric response and the concentrations of these analytes yielded linear calibration curves (r^2 = 0.99). The method detection limits (MDL) for H_2O_2, RhB, and Fe were 0.08 mg/L, 0.0015 mg/L and 0.03 mg/L, respectively. All samples were analyzed in replicate or triplicate. The pH was measured using the Orion Star A215 pH meter (EPA Method 150.1). The 95% confidence intervals were used as a statistical metric to assess the range of potential values of the measured parameter.

3. Results and discussion

3.1. Solids characterization

The specific surface area of silica and alumina was significantly less than MMT (Table 2). The pH point of zero charge (pH_{PZC}) of alumina was greater than silica and MMT (Table 2) indicating it carried a net positive charge over the pH range relative to silica and MMT. Greater concentrations of Fe and Mn in MMT explain the mineral's reactivity with H_2O_2. XRD patterns of the minerals tested were consistent with the diffraction patterns found in the library of available mineral (S.2, Figure S2).

The $[Si]_{AQUEOUS}$ in the acidified suspensions of silica (0.057 mg/L Si) and alumina (0.017 mg/L Si) were below the detection limit (0.1 mg/L). The $[Si]_{AQUEOUS}$ in the acidified re-suspensions of silica (0.004 mg/L Si) and alumina (0.013 mg/L Si) were lower indicating that silica leaching from SiO_2 and Al_2O_3 was negligible or did not occur altogether. This indicates that dissolved silica had a negligible inhibitory effect on the H_2O_2 activation in this system. Additionally, Visual MINTEQ ver. 3.1 (Gustafsson, 2014) was applied to determine the Fe^{3+} speciation under reaction conditions in the Fe-AHP (i.e., pH 3.5,1 h). $Fe(OH)^{2+}$ (~63%) and $Fe(OH)_2^+$ (~34%) were identified as the predominant iron species. Possibly, these deprotonated Fe^{3+} complexes were loosely attracted to the solid surfaces. However, the fate of H_2O_2 was not impacted by the presence of these minerals as discussed in section 3.2.

3.2. Summary of experimental controls

Comprehensive control experiments were conducted to evaluate potential fate mechanisms for RhB, H_2O_2, and •OH (S.3; Figures S3 – S9) and confirmed that oxidative transformation by •OH was the only significant fate mechanism of RhB. H_2O_2 decomposition (11–13%) was similar between the base-case un-amended homogeneous system (Fe^{3+}+H_2O_2+RhB), and all reaction systems containing alumina and silica, indicating that Fe^{3+} was the only activator of H_2O_2. The H_2O_2 degradation rate (k_{H2O2}) in silica-and alumina-amended reactors was 3.58×10^{-5} 1/s (95% confidence interval (C.I.) = 3.22×10^{-5}–3.95×10^{-5} 1/s; n = 8) and 3.17×10^{-5} 1/s (95% C.I. = 2.45×10^{-5}–3.88×10^{-5} 1/s; n = 3), respectively. In the mineral-free, homogeneous case it was 3.75×10^{-5} 1/s (95% C.I. = 2.69×10^{-5}–4.81×10^{-5} 1/s; n = 3). Therefore, k_{H2O2} was not statistically distinguishable (95% confidence)

between the treatment systems, and that the rates of •OH production (P_{OH}) were equal between mineral-free and mineral-amended reactors (Table S1).

3.3. Scavenging of •OH by solid surfaces in heterogenous systems

3.3.1. Silica and alumina (unreactive with H_2O_2) in Fe-AHP systems—The least-square regression of semi-logarithmic plots of RhB concentration versus time were linear, indicating that •OH concentrations were at steady-state ($[•OH]_{SS}$) and were used to determine the pseudo-first order degradation rate constants for RhB (k_{RhB}) (Table 3). In the solids-amended Fe-AHP system, RhB oxidative losses were inversely proportional with silica and alumina solids (S.4, Figure S10), and k_{RhB} progressively declined with increasing silica or alumina.

(Table 3). k_{RhB} were used to calculate $[OH]_{SS}$ (Eq. (10)) in systems containing silica or alumina (Table 3). k_S, the sum of products of individual aqueous phase scavengers (S_i) and respective •OH reaction rate constants (k_i) (Eq. (7)), was estimated as, 2.7×10^7 (1/M × s) × $[H_2O_2]$, since •OH reaction with H_2O_2 was significantly greater than all other aqueous phase scavenging reactions. $k_{≡S}$ was calculated by contrasting laboratory-derived kinetic parameters between the base-case, solids-free, homogenous systems, and the solids-amended heterogeneous systems (Eq. (13)). The average value of $k_{≡S}$ for silica (2.85×10^6 $1/m^2 \times s$; n = 10) was not statistically distinguishable at the 95% confidence level from alumina (3.92×10^6 $1/m^2 \times s$; n = 7) (Table 3).

$k_{≡S}$ was also estimated by contrasting RhB reaction kinetics between two solids-amended, heterogeneous oxidative systems containing differing quantities of the same mineral (Eq. (16)). The average value of $k_{≡S}$ for silica was 2.55×10^6 $1/m^2 \times s$ (95% C.I.= 5.7×10^5–4.5×10^6 $1/m^2 \times s$; n = 9) (Table S2) and was consistent with $k_{≡S}$ using Eq. (13) (i.e., 12% difference). The scavenging rate ($k_{≡S} \times S_A \times m_S \times [•OH]_{SS}$ (mol/L × s)) was asymptotic with increasing alumina and silica concentrations (Figure S11). At higher solids content, the overall scavenging rate increased, but the incremental change in rate of •OH scavenging decreased. These incremental differences, as reflected in the kinetic parameters k_{RhB} and $[OH]_{SS}$, made it increasingly difficult to accurately estimate $k_{≡S}$. Consequently, estimates of $k_{≡S}$ (Eq. (16)) are less accurate when contrasting treatment systems containing higher solids concentrations.

The initial rates of •OH reaction with RhB, H_2O_2, and silica or alumina were contrasted to assess the relative fate of •OH (Fig. 1). At low concentrations of silica or alumina, H_2O_2 was the predominant scavenger, but minerals were the more predominant scavengers at 10 g/L and higher. Results indicate that silica and alumina mineral surfaces scavenge •OH, that mineral surfaces play a significant role in the fate of •OH, and that surface scavenging represents a major source of treatment inefficiency in Fe-AHP systems.

3.3.2. Mineral surface scavenging in UV-AHP systems—In the UV-AHP system, the average pH of all mineral suspensions was near neutral (pH 6.8). The H_2O_2 decomposition (11–13%) was similar between the mineral-free system and reaction systems containing alumina and silica indicating that UV was the only activator of H_2O_2. k_{H2O2} in silica- and alumina-amended reactors was 1.16×10^{-5} 1/s (95% C.I. =1.03×10^{-5}–$1.29 \times$

10^{-5} 1/s; n = 2) and 1.21×10^{-5} 1/s (95% C.I. = 1.14×10^{-5}–1.29×10^{-5} 1/s; n = 9), respectively. In the mineral-free, homogeneous case it was 1.34×10^{-5} 1/s (95% C.I. = 1.12×10^{-5}–1.56×10^{-5} 1/s; n = 4). These results indicated that k_{H2O2} was not statistically distinguishable (95% confidence) between these treatment systems and that P_{OH} was approximately equal between mineral-free and mineral-amended reactors. The H_2O_2 reaction rate increased linearly with [MMT] (1–50 g/L) (Table S1). Average $k_{\equiv S}$ values for silica (4.50×10^6 1/m^2 × s; n = 2) and alumina (7.45×10^6 1/m^2 × s; n = 11), were greater by factors of 1.6 and 1.9 over $k_{\equiv S}$ estimates in the Fe-AHP system (Table 3). Similar variability is reported for rate constants involving reactions of radicals in aqueous solutions and may involve various sources of error (Buxton et al., 1988). $k_{\equiv S,MMT}$ ($\leq 4.22 \times 10^5$ 1/m^2 × s; n = 8) was 11–18 times less than $k_{\equiv S}$ for silica and alumina, respectively. The general trend was $k_{\equiv S,silica} \sim k_{\equiv S,alumina} > k_{\equiv S,MMT}$.

3.3.3. Impact of $k_{\equiv S}$ in remediation of unconsolidated porous media—

Contrasting •OH reaction rates with naturally occurring reactants found in aquifer material, dissolved scavenger species, and a target contaminant provides insight regarding the impact of surface scavenging on remediation of soil and groundwater contaminants associated with ISCO treatment systems. In subsurface systems, the solids to water ratio is much greater than in the dilute suspensions used during the laboratory testing. This suggests the rate of •OH scavenging by mineral surfaces could be much greater in aquifer and soil systems than in the mineral suspensions used in this study. •OH scavenging rates were calculated using experimentally-derived values of $k_{\equiv S}$ (Table 2) and were contrasted with •OH reaction rates with aqueous phase species. In this analysis, conditions and parameter values were assumed and included an ideal representative volume of unconsolidated porous media (1 m^3), 1 pore volume mixture of trichloroethylene (TCE) (10 mg/L) and H_2O_2 (10 g/L) with instantaneous mixing, no TCE sorption, and $[\bullet OH]_{SS} = 5 \times 10^{-16}$ mol/L (Fig. 2). The rate of •OH reaction with solid surfaces (t = 0 h) dominated the fate of •OH by several orders of magnitude, relative to TCE and H_2O_2 in the aqueous phase (Fig. 2). These results underscore the dominant role of surface scavenging when Fe-AHP oxidative treatment is carried out in soil and aquifer systems.

Hydrophobic organic compounds adsorbed to solid phase media may be incapable of reacting with •OH because •OH react with dissolved species faster than the •OH can diffuse across the solid-liquid interface to react with adsorbed compounds (Sedlak and Andren, 1994). Conversely, in our study, •OH reaction was dominated by surface scavenging at 10–50 g/L silica, alumina, or MMT, in both Fe-AHP and UV-AHP systems (Fig. 1), and even greater •OH scavenging was projected under unconsolidated porous media conditions (Fig. 2). These contrasting results are provocation to explore revisions to the heterogeneous oxidative treatment system conceptual model. It is assumed solid phase mineral surfaces are comprised of intermingled sorption and scavenging sites. During oxidative treatment, competition kinetics between •OH surface scavenging and •OH oxidation of sorbed and/or aqueous phase contaminants, is functionally dependent on several variables including the number of scavenging and sorption sites. The surface scavenging rate constant, $k_{\equiv S}$ (1/m^2 × s), is simplified as $\Sigma_{i=1}^{n} k_{\equiv,i} \times [S_{\equiv,i}]$ (Eq. (8)) where $k_{\equiv,i}$ (L/mol × s) is the specific second-order reaction rate constant between •OH and individual specific solid phase

scavengers $S_{\equiv,i}$ (mol/L × m^2) (i.e., surface scavenger sites). Since •OH reacts at near diffusion-controlled rates, •OH transport is limited to a few nanometers from where it was formed. This suggests the dominant role of surface radical scavenging must be attributed to the abundance of $S_{\equiv,i}$ on solid surfaces.

Currently, although $k_{\equiv,i}$ is not well understood and not quantified, it may be correlated with the concentration of hydroxyl ions (•OH) on solid surfaces, a known reactant of •OH (Sedlak and Andren, 1994; Suh et al., 2000) (1.2×10^{10} 1/M × s) (Buxton et al., 1988). This may also explain greater estimates of $k_{\equiv S}$ in UV-AHP systems (pH 6.8), where a greater abundance of OH^- occurred on the surface relative to Fe-AHP systems (pH 3.5) (Table 2). It is not proposed that Si nor Al specifically scavenge •OH, as these elements exhibit their highest oxidation state. Rather, the abundance of surface hydroxyl groups or surface defect sites formed during the synthesis dehydration step can serve as potential electron donors and surface scavenging sites (Suh et al., 2000; Flockhart et al.,1970; Konency, 2001). It is proposed that the oxidation of sorbed compounds on solid surfaces can be limited by the relative abundance of scavenging sites to sorption sites, and consequently, the high rate of •OH reaction at scavenging sites relative to sorption sites. Aggressive •OH surface scavenging, as demonstrated in this study, provided a plausible explanation why organic compounds become less vulnerable to oxidative treatment in heterogeneous systems when adsorbed to solid surfaces.

UV photoactivation of titanium dioxide (TiO_2) nanoparticles (TiO_2-NP) produces •OH and serves as the fundamental mechanism for oxidative treatment used in environmental applications (Pelaez et al., 2012). A wide range of TiO_2-NP support media includes alumina clays, alumina ceramics, zeolites, glass products (i.e., silica dioxide) (Puma et al., 2008). The results of this study suggest these materials would likely exhibit significant •OH surface scavenging characteristics. It is recommended that one of the underlying criteria for selecting an ideal catalyst support is that the media should be optimally inert with respect to •OH scavenging. Utilizing methods developed and reported in this study to quantify $k_{\equiv S}$ could be used to screen the candidate support media.

4. Conclusions

- A kinetic analysis model was developed to differentiate between radical scavenging in the aqueous and solid phases, and to estimate solid surface radical scavenging rate constants ($k_{\equiv S}$).
- Two of the minerals tested, silica and alumina, did not react with H_2O_2; montmorillonite reacted with H_2O_2 but did not produce •OH. Two oxidative treatment systems were used to determine $k_{\equiv S}$ including the Fe-activated H_2O_2 system (Fe-AHP) and the UV-activated H_2O_2 system (UV-AHP).
- In the Fe-AHP system, $k_{\equiv S}$ for silica (2.85×10^6 1/m^2 × s) and alumina (3.92×10^6 1/m^2 × s) were similar. In the UV-AHP system, estimates of $k_{\equiv S}$ for silica (4.50×10^6 1/m^2 × s) and alumina (7.45×10^6 1/m^2 × s) were higher and was attributed to the higher pH in the UV-AHP system. $k_{\equiv S}$ for montmorillonite in

the UV-AHP system was ≤4.22×10^5 $1/m^2 \times s$; overall, $k_{\equiv S,silica} \sim k_{\equiv S,alumina} > k_{\equiv S,MMT}$ indicating $k_{\equiv S}$ is mineral specific.

- Low concentrations of silica or alumina (10 g/L) scavenged •OH at rates greater than the reaction rate with H_2O_2, a well-known scavenger of •OH, and the target compound, RhB.
- Assuming in-situ chemical oxidation (ISCO) treatment conditions, experimentally-derived •OH scavenging rate constants were used to contrast •OH reaction rates with various reactants in unconsolidated porous media. •OH reaction was dominated by solid surfaces comprised of silica, alumina, and montmorillonite minerals relative to •OH reaction with trichloroethylene, the target compound, and H_2O_2, a well-documented radical scavenger. These results indicate that solid mineral surfaces play a key role in limiting treatment efficiency in ISCO systems.

Supplementary Material

Refer to Web version on PubMed Central for supplementary material.

Acknowledgements

The Authors acknowledge L. Callaway, L. Costantino, M. Sexton, Dr. C. Su, M. White (US EPA, R.S. Kerr Environmental Research Center), Dr. B. Pivetz (CSS, Buffalo, NY), J. Brown (Oak Ridge Associated Universities, Ada, OK) and Constance Green (East Central University, Ada, OK) for analytical and technical support.

Notice

The views expressed in this journal article are those of the authors and do not necessarily represent the views and policies of the U.S. Environmental Protection Agency. The U.S. Environmental Protection Agency, through its Office of Research and Development, funded and managed the research described here.

References

APHA, AWWA, WEF, 1989 In: Clesceri LS, Greenberg AE, Trussell RR (Eds.), Method 3500-Fe D. Phenanthroline Method, seventeenth ed 3-102–3-106.

Babuponnusami A, Muthukumar K, 2014 A review on Fenton and improvements to the Fenton processes for wastewater treatment. J. Environ. Chem. Eng 2, 557–572.

Baldrian P, Merhautova V, Gabriel J, Nerud F, Stopka P, Hruby M, Benes MJ, 2006 Decolorization of synthetic dyes by hydrogen peroxide with heterogeneous catalysis by mixed iron oxides. Appl. Catal. B Environ 66 (3–4), 258–264.

Bautista P, Mohedano AF, Casas JA, Zazo JA, Rodriguez JJ, 2008 An overview of the application of Fenton oxidation to industrial wastewaters treatment. J. Chem. Technol. Biotechnol 83, 1323–1338.

Buxton GV, Greenstock CL, Helman WP, Ross AB, 1988 Critical-review of rate constants for reactions of hydrated electrons, hydrogen-atoms and hydroxyl radicals (•OH/O•−) in aqueous-solution. J. Phys. Chem. Ref. Data 17, 513–886.

Flockhart BD, Leith IR, Pink RC, 1970 Electron-transfer at alumina surfaces. Part 3. Reduction of aromatic nitro-compounds. Trans. Faraday Soc 66, 469–476.

Garrido-Ramirez EG, Theng BKG, Mora ML, 2010 Clays and oxide minerals as catalysts and nanocatalysts in Fenton-like reactions – a review. Appl. Clay Sci 47, 182–192.

Grebel JE, Pignatello JJ, Mitch WA, 2010 Effect of halide ions and carbonates on organic contaminant degradation by hydroxyl radical-based advanced oxidation processes in saline waters. Environ. Sci. Technol 44 (17), 6822–6828. [PubMed: 20681567]

Gustafsson JP, 2014 Visual MINTEQ 3.1. Retrieved 05-05, 2014, from. http://www2.lwr.kth.se/English/Oursoftware/vminteq/download.html.

Haag WR, Yao CCD, 1992 Rate constants for reaction of hydroxyl radicals with several drinking water contaminants. Environ. Sci. Technol 26 (5), 1005–1013.

Hermanek M, Zboril R, Medrik I, Pechousek J, Gregor C, 2007 Catalytic efficiency of iron(III) oxides in decomposition of hydrogen peroxide: Competition between the surface area and crystallinity of nanoparticles. J. Am. Chem. Soc 129 (35), 10929–10936. [PubMed: 17691785]

Huang HH, Lu MC, Chen JN, 2001 Catalytic decomposition of hydrogen peroxide and 2-chlorophenol with iron oxides. Water Res. 35 (9), 2291–2299. [PubMed: 11358310]

Huling SG, Arnold RG, Sierka RA, Miller MR, 1998 Measurement of hydroxyl radical activity in a soil slurry using the spin trap α-(4-pyridyl-1-oxide)-N-tert-butyl nitrone. Environ. Sci. Technol 32, 3436–3441.

Huling SG, Arnold RG, Sierka RA, Miller MR, 2001 Influence of peat on Fenton oxidation. Water Res. 35 (7), 1687–1694. [PubMed: 11329670]

Huling SG, Pivetz B, 2006 In-situ Chemical Oxidation - Engineering Issue. EPA/600/R-06/072.

Konency R, 2001 Reactivity of hydroxyl radicals on hydroxylated quartz surface. 1. Cluster model calculations. J. Phys. Chem. B 105, 6221–6226.

Kwan WP, Volker BM, 2002 Decomposition of hydrogen peroxide and organic compounds in the presence of dissolved iron and ferrihydrite. Environ. Sci. Technol 36, 1467–1476. [PubMed: 11999052]

Kwan WP, Volker BM, 2003 Rates of hydroxyl radical generation and organic compound oxidation in mineral-catalyzed Fenton-like systems. Environ. Sci. Technol 37 (6), 1150–1158. [PubMed: 12680668]

Luo M, Bowden D, Brimblecombe P, 2009 Catalytic property of Fe-Al pillared clay for Fenton oxidation of phenol by H_2O_2. J. Appl. Catal. B: Environ. Times 85, 2010–2206.

Matta R, Hanna K, Chiron S, 2007 Fenton-like oxidation of 2,4,6-trinitrotoluene using different iron minerals. Sci. Total Environ 385, 242–251. [PubMed: 17662375]

Miller CM, Valentine RL, 1999 Mechanistic studies of surface catalyzed H_2O_2 decomposition and contaminant degradation in the presence of sand. Water Res. 33, 2805–1816.

Navalon S, Alvaro M, Garcia H, 2010 Heterogeneous Fenton catalysts based on clays, silicas and zeolites. J. Appl. Catal. B: Environ. Times 99 (1–2), 1–26.

Pelaez M, Nolan NT, Pillai SC, Seery MK, Falaras P, Kontos AG, Dunlop PSM, Hamilton JWJ, Byrne JA, O'Shea K, Entezari MH, Dionysiou DD, 2012 A review on the visible light active titanium dioxide photocatalysts for environmental applications. J. Appl. Catal. B: Environ. Times 125, 331–349.

Petigara BR, Blough NV, Mignerey AC, 2002 Mechanisms of hydrogen peroxide decomposition in soils. Environ. Sci. Technol 36 (4), 639–645. [PubMed: 11878378]

Pham AL, Lee C, Doyle FM, Sedlak DL, 2009 A silica-supported iron oxide catalyst capable of activating hydrogen peroxide at neutral pH values. Environ. Sci. Technol 43, 8930–8935. [PubMed: 19943668]

Pignatello JJ, Oliveros E, MacKay A, 2006 Advanced oxidation processes for organic contaminant destruction based on the Fenton reaction and related chemistry. Crit. Rev. Environ. Sci. Technol 36 (1), 1–83.

Puma GL, Bono B, Krishnaiah D, Collin JG, 2008 Preparation of titanium dioxide photocatalyst loaded onto activated carbon support using chemical vapor deposition: a review paper. J. Hazard Mater 157, 209–219. [PubMed: 18313842]

Remucal CK, Sedlak DL, 2011 The role of iron coordination in the production of reactive oxidants from ferrous iron oxidation by oxygen and hydrogen peroxide. Aquatic Redox Chemistry. Chapter 9, pp. 177–197.

Rusevova K, Kopinke FD, Georgi A, 2012 Nano-sized magnetic iron oxides as catalysts for heterogeneous Fenton-like reactions - influence of Fe(II)/Fe(III) ratio on catalytic performance. J. Hazard Mater 241–242, 433–440.

Schwarzenbach RP, Gschwend PM, Imboden DM, 2003 Environmental Organic Chemistry, second ed Wiley-Interscience.

Sedlak DL, Andren AW, 1994 The effect of sorption on the oxidation of polychlorinated biphenyls (PCBs) by hydroxyl radical. Water Res.28 (5), 1207–1215.

Sheng Y, Sun Y, Ju X, Zhang J, Han YF, 2017 Fenton-like degradation of Rhodamine B over highly durable Cu-embedded alumina: kinetics and mechanism. AIChE J. 64 (2), 538–549.

Siegrist RL, Crimi M, Simpkin TJ, 2011 Situ Chemical Oxidation for Groundwater Remediation. Springer-Verlag, New York.

Suh M, Bagus PS, Pak S, Rosynek MP, Lunsford JH, 2000 Reactions of hydroxyl radicals on titania, silica, alumina, and gold surfaces. J. Phys. Chem. B 104, 2736–2742.

Xu X, Thomson NR, 2010 Hydrogen peroxide persistence in the presence of aquifer materials. Soil Sediment Contam. 19, 602–616.

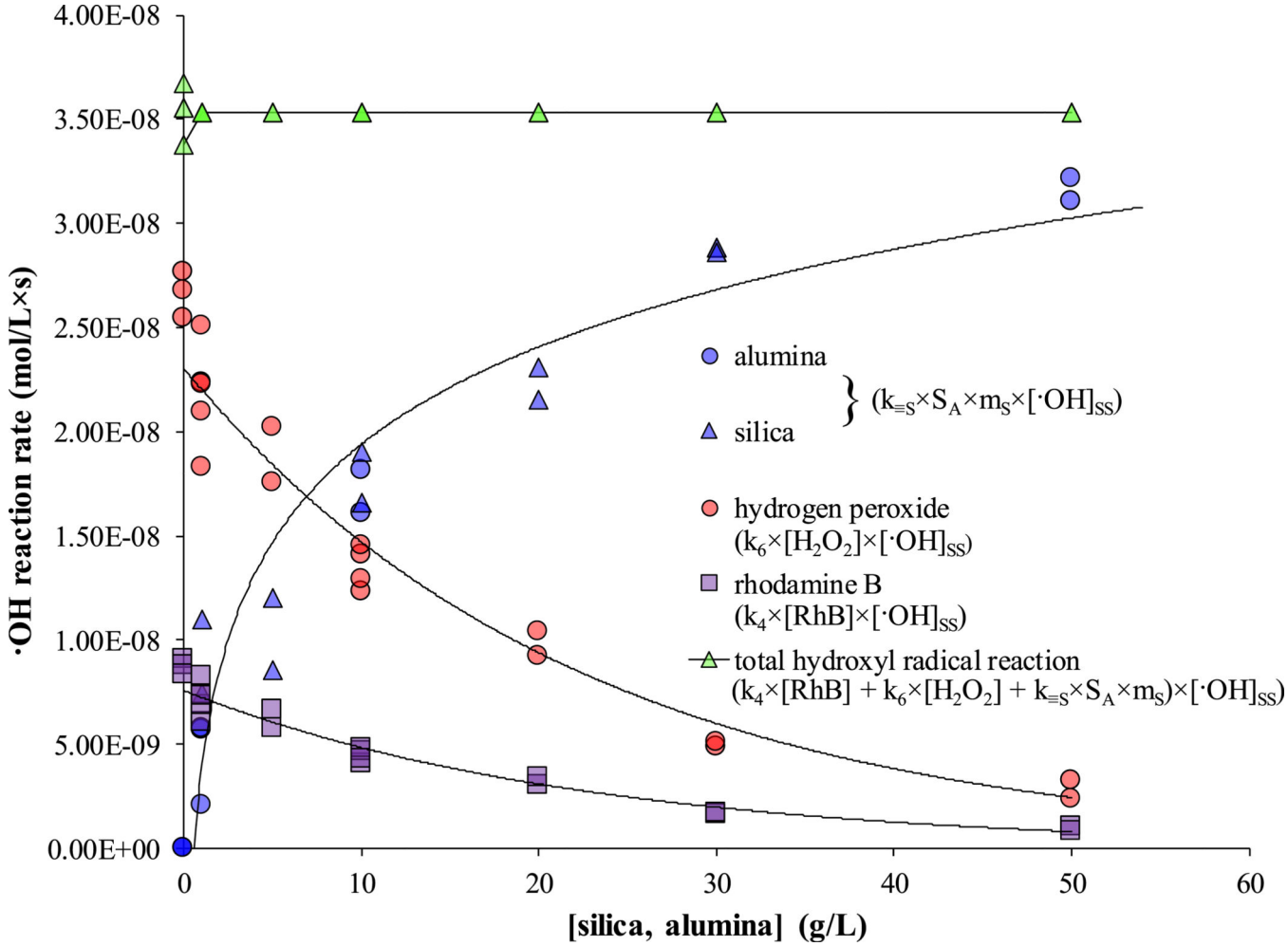

Fig. 1.

The initial •OH reaction rates with RhB (5 mg/L; 1.04×10^{-2} mmol/L), H_2O_2 (1000 mg/L; 2.94 mmol/L), and silica (0–30 g/L) or alumina (0–50 g/L).

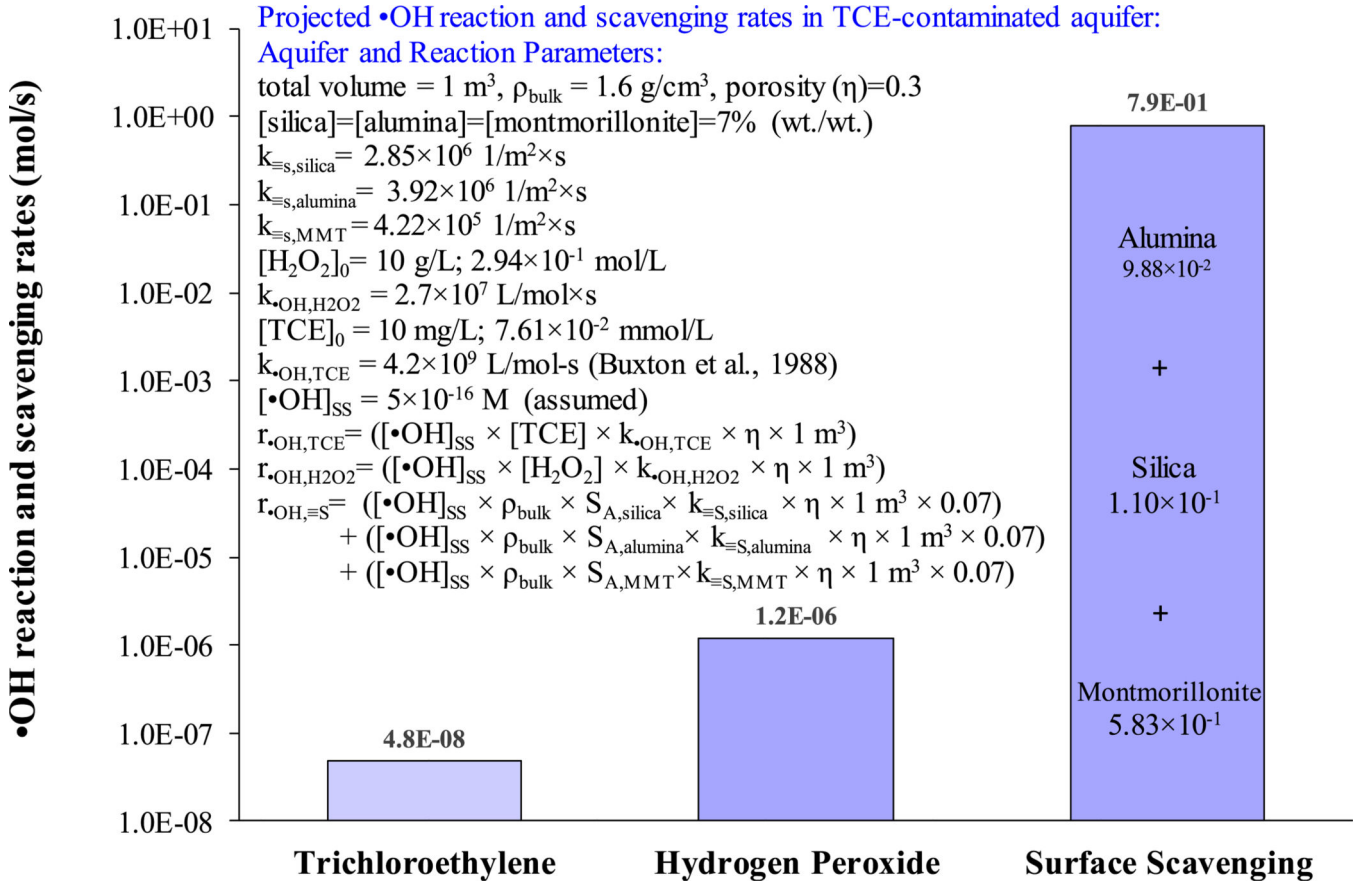

Fig. 2.

Calculated •OH reaction and scavenging rates in aquifer material where scavenging rate constants were used from this study.

Table 1

Hydrogen peroxide-based oxidation reactions.

H_2O_2 activation and related reactions.	
$H_2O_2 + Fe^{2+} \rightarrow Fe^{3+} + OH^- + \bullet OH$	R 1
$H_2O_2 + Fe^{3+} \rightarrow Fe^{2+} + \bullet O_2^- + 2H^+$	R 2
$\bullet O_2^- + Fe^{3+} \rightarrow Fe^{2+} + O_2$	R 3
$\bullet OH + RhB \rightarrow$ products $k_4 = 2.5 \times 10^{10}$ 1/M × s (Buxton et al., 1988)	R 4
$\bullet OH + \Sigma_{i=1}^{n} [S_i] \rightarrow$ products	R 5
$\bullet OH + H_2O_2 \rightarrow HO_2\bullet^- + H_2O$ $k_6 = 2.7 \times 10^7$ 1/M × s (Buxton et al., 1988)	R 6
$\bullet OH + \equiv S_i \rightarrow$ products	R 7
$2H_2O_2 \xrightarrow{\text{Mn- and some Fe-oxides}} O_2 + H_2O$	R 8
$2H_2O_2 \xrightarrow{\text{Fe-oxide}} \bullet OH_2 + HO_2\bullet^- + H_2O$	R 9
$H_2O_2 \xrightarrow{\text{UV}} 2 \bullet OH$	R 10

Note: $\Sigma_{i=1}^{n} [S_i]$ is the pseudo-first-order rate constant (k_S 1/s) for •OH scavenging by all constituents in solution except the target compound.

Table 2

Characterization results for silica, alumina, and montmorillonite (MMT) minerals used as •OH scavengers in Fe-AHP and UV-AHP oxidation experiments.

Mineral	Specific Surface[a] Area (m^2/g)	pH_{PZC} [b]	Fe_{Total} (mg/kg)	Mn_{Total} (mg/kg)
Silica	2.3 ± 0.2	2.0	238	BQL[c]
Alumina	1.5 ± 0.3	8.5	19	BQL[c]
MMT	82.2 ± 3.5	2.5	8065	248

[a] silica (n = 3); alumina (n = 8); MMT (n = 6).

[b] Schwarzenbach et al. (2003).

[c] BQL = below quantitation limit (8.1 mg/kg for Mn, 4.0 mg/kg for Fe).

Table 3

Estimates of the surface scavenging rate constants ($k_{\equiv S}$) using Eq. (13) (S.1) for silica, alumina, and montmorillonite in Fe-AHP and UV-AHP treatment systems.

[mineral] (g/L)	k_{RhB} [a] (1/s)	$[•OH]_{SS}$ [a] (mol/L)	$k_{\equiv S}$ [a] ($1/m^2 \times s$)
Fe-AHP [b]			
silica			
0 (n = 3)	8.37×10^{-4}	3.35×10^{-14}	–
1 (n = 2)	6.18×10^{-4}	2.48×10^{-14}	6.61×10^{6}
5 (n = 2)	5.93×10^{-4}	2.38×10^{-14}	1.53×10^{6}
10 (n = 2)	4.15×10^{-4}	1.66×10^{-14}	1.88×10^{6}
20 (n = 2)	3.08×10^{-4}	1.24×10^{-14}	1.58×10^{6}
30 (n = 2)	1.57×10^{-4}	6.27×10^{-15}	2.66×10^{6}
			Avg. 2.85×10^{6}
alumina			
0 (n = 3)	8.37×10^{-4}	3.35×10^{-14}	–
1 (n = 3)	7.31×10^{-4}	2.92×10^{-14}	4.15×10^{6}
10 (n = 2)	4.32×10^{-4}	1.73×10^{-14}	2.64×10^{6}
50 (n = 2)	8.83×10^{-5}	3.54×10^{-15}	4.86×10^{6}
			Avg. 3.92×10^{6}
UV-AHP [c]			
silica			
0 (n = 3)	4.09×10^{-4}	1.64×10^{-14}	–
1 (n = 1)	3.28×10^{-4}	1.31×10^{-14}	4.50×10^{6}
10 (n = 1)	1.19×10^{-4}	4.74×10^{-15}	4.50×10^{6}
			Avg. 4.50×10^{6}
alumina			
0 (n = 3)	4.09×10^{-4}	1.64×10^{-14}	–
1 (n = 3)	2.99×10^{-4}	1.20×10^{-14}	1.10×10^{7}
5 (n = 2)	1.55×10^{-4}	6.20×10^{-15}	9.17×10^{6}
10 (n = 3)	1.18×10^{-4}	4.73×10^{-15}	7.02×10^{6}
50 (n = 3)	6.17×10^{-5}	2.47×10^{-15}	3.21×10^{6}
			Avg. 7.45×10^{6}
montmorillonite			
0 (n = 3)	4.09×10^{-4}	1.64×10^{-14}	–
1 (n = 2)	1.38×10^{-4}	5.50×10^{-15}	$\leq 1.01 \times 10^{6}$
5 (n = 2)	8.67×10^{-5}	3.47×10^{-15}	$\leq 3.82 \times 10^{5}$
10 (n = 2)	7.25×10^{-5}	2.90×10^{-15}	$\leq 2.38 \times 10^{5}$
50 (n = 2)	5.83×10^{-5}	2.33×10^{-15}	$\leq 6.17 \times 10^{4}$
			Avg. $\leq 4.22 \times 10^{5}$

[a] Average k_{RhB} and $[\bullet OH]_{SS}$ for mineral phase concentrations 0–50 g/L; k_{RhB} in the Fe-AHP system $0.93 \leq r^2 \leq 0.99$; k_{RhB} in the UV-AHP system $0.94 \leq r^2 \leq 0.99$.

[b] *Fe-AHP system:* Average $k_{\equiv S}$ (n = 10) using 1–30 g/L silica (95% C.I. = 1.29×10^6–4.42×10^6 $1/m^2 \times s$); average $k_{\equiv S}$ (n = 7) using 1–50 g/L alumina (95% C.I. = 2.44×10^6–5.41×10^6 $1/m^2 \times s$).

[c] UV-AHP system: Average $k_{\equiv S}$ (n = 2) using 1–10 g/L silica (95% C.I. = 4.47×10^6–4.53×10^6 $1/m^2 \times s$; average $k_{\equiv S}$ (n = 11) using 1–50 g/L alumina (95% C.I. = 7.29×10^6–7.61×10^6 $1/m^2 \times s$); average $k_{\equiv S}$ (n = 8) using 1–50 g/L montmorillonite ($\geq 1.02 \times 10^5$–7.42×10^5 $1/m^2 \times s$).